sensors

MDPI

Article

Genetic Deep Convolutional Autoencoder Applied for Generative Continuous Arterial Blood Pressure via Photoplethysmography

Muammar Sadrawi [1], Yin-Tsong Lin [2], Chien-Hung Lin [2], Yita Hsieh[2], Bhekumuzi Mathunjwa [1], Shou-Zen Fan [3], Maysam F. Abbod [4] and Jiann-Shing Shieh [1,*]

[1] Department of Mechanical Engineering and Innovation Center for Big Data and Digital Convergence, Yuan Ze University, Taoyuan, Chung-Li 32003, Taiwan; muammarsadrawi@yahoo.com (M.S); mathunjwabhekie@gmail.com (B.M)

[2] Healthcare and Beauty RD Center, Kinpo Electronics, Inc., New Taipei City 222, Taiwan; lotusytlin@neweraai.com (Y.-T.L.); lance_lin@kinpo.com.tw (C.-H.L.); yita_hsieh@calcomp.com.tw (Y.H.)

[3] Department of Anestheology, College of Medicine, National Taiwan University, Taipei 100, Taiwan; shouzen@gmail.com

[4] Department of Electronic and Computer Engineering, Brunel University London, Uxbridge UB8 3PH, UK; Maysam.Abbod@brunel.ac.uk

* Correspondence: jsshieh@saturn.yzu.edu.tw

Abstract: Hypertension affects huge number of people around the world. It also has a great contribution to cardiovascular and renal related diseases. This study investigates the ability deep convolutional autoencoder (DCAE) to generate the continuous arterial blood pressure (ABP) by only utilizing the photoplethysmography (PPG) to generate the continuous ABP. The total of 18 patients is utilized. LeNet-5 and U-Net based DCAEs, respectively for LDCAE and UDCAE, are compared to the MP60 IntelliVue Patient Monitor, as the golden standard. Moreover, in order to investigate the data generalization, leave-one-out cross-validation (CV) method is conducted. The results show that the UDCAE provides superior results in producing the SBP estimation. Meanwhile, LDCAE gives a slightly better for the DBP prediction. Finally, the genetic algorithm (GA) based optimization deep convolutional autoencoder (GDCAE) is further administered to optimize the ensemble of the CV models. The results reveal that the GDCAE is superior to either the LDCAE or UDCAE. For conclusion, this study reveals that the SBP and DBP can also be accurately achieved by only utilizing the single PPG signal.

Keywords: photoplethysmography; continuous arterial blood pressure; systolic blood pressure; diastolic blood pressure; deep convolutional autoencoder; genetic algorithm

1. Introduction

According to World Health Organization (WHO), blood pressure (BP) is the pressure driven by the blood circulation to the artery wall. Meanwhile, the hypertension or high blood pressure (HBP) is the excessive amount of the given force against blood vessels. In further, WHO also stated that HBP affects more than one billion people in the world [1].

With having impact to many people, HBP in further can incite several diseases. It has solid contribution to cardiovascular and renal diseases [2]. HBP also contributed to stroke and ischemic heart diseases [3]. Furthermore, HBP can generate vascular damage of retina related to the cardiovascular-related fatality [4]. These aforementioned studies make the HBP-related inspection, utilizing the other vital signs, become significant.

Photoplethysmography (PPG), one of the vital signs, has been a solid indicator for some medical-related investigations. PPG has been deployed as the heart rate measurement in the motion artifact-interfered condition with empirical mode decomposition-based filter and time-frequency evaluation [5]. It also has been utilized, alongside electrocardiography, for the atrial fibrillation in acute stroke patient [6]. Another study has involved the PPG morphological feature for the hypertension early identification [7]. Moreover, Phillips et. al., applied the PPG sensors to non-invasively evaluate the hemoglobin concentration [8]. Meanwhile, Perpetuini et. al., supervised the general linear model-based PPG to evaluate the ankle-brachial index, which was initially measured using commercial instrument as the golden standard [9]. In another case, lately, entropy-based PPG evaluations have been successfully distinguished between healthy and diabetic patients [10].

There are specifically assorted previous studies that effectively demonstrated the substantial interconnection between PPG and BP. A study investigated the relationship of the PPG with intermittent systolic and diastolic blood pressures using multi-scale entropy and ensemble neural network [11]. Sideris et. al., evaluated the continuous arterial blood pressure (ABP) using long-short term memory (LSTM) from patients in intensive care unit (ICU) using the only PPG signal [12]. Furthermore, the hybrid of LSTM and artificial neural network (ANN) were performed via ECG and PPG to measure the BP [13]. In further, autoregressive moving average to investigate the blood pressure also by using features of PPG signal with related to the specific breathing conditions was performed and showed a quality evaluation [14]. Meanwhile, multiple signals from ECG, PPG and ballistocardiograms (BCG) were used to investigate the systolic blood pressure (SBP) and diastolic blood pressure (DBP) by utilizing hybrid artificial intelligence (AI) methods [15].

Recently, AI has been widely used in many fields. It has been used simultaneously with computational fluid dynamics in order to optimize the control scheme by adjusting the triangular membership function for the cooling system in a heat exchanger [16]. The hybrid AI, combining the extreme learning machine with cuckoo search algorithm, was applied for biodiesel production [17]. Meanwhile, a

study used neural network with multi-armed bandit algorithm for solid oxide fuel cell problem [18]. Moreover, Zaidan et. al., applied the AI model for the gas turbine engine inspection [19].

Specifically to medical-related studies, ANN has been used for detecting depth of anesthesia with involving multi-vital signs [20]. This previous study applied the entropy-based calculation to extract the feature from one vital sign, which is the EEG. Meanwhile, the 5-second intermittent data from other vital signs were later combined with the extracted entropy value from the EEG. Finally, the cross-validation technique was used to evaluate the data generalization when dealing with data shuffling for the training season. A wearable device-related study also utilized ANN in classifying arrhythmia [21]. Fast Fourier transform (FFT) was also administered to evaluate one of the arrhythmia in the frequency domain evaluation. Moreover, The ANN model was also implemented to predict the pneumonia [22, 23].

Besides being utilized for the generalization evaluation [20], the ensemble technique is likely used to increase the accuracy of the models. However, selecting all the models for the ensemble system has not always been the best solution [24]. The combination of the fuzzy clustering, ANN and genetic algorithm (GA), was administered for ensemble model for the highly unbalanced data evaluation in emergency medical service [25]. The GA was called to investigate which models should be allocated to have a good ensemble mode. Furthermore, this related study examined the quality of the model best on the area under the curve (AUC) from the receiver operating characteristic (ROC) as the fitness function. The result from this study [25] convincingly supported the study by Zhou, Z.H. et. al [24]. The ensemble model definitely will increase the result. Nevertheless, selecting several classifiers is likely to produce a better result than combining all of them [24].

Recently, the neural network method tends to move towards the deeper structure, called deep neural network [26]. This system has been administered to the substantial studies. One of the methods, the convolutional neural network (CNN), has been used to predict the arrhythmia with very precise result with comparison to cardiologist [27]. Another powerful evidence by the CNN based evaluation technique has also been performed to solve the seizure problem using encephalogram (EEG) [28]. Moreover, a study evaluated the depth of anesthesia that utilizing short time Fourier transform (STFT) and CNN [29] was investigated to evaluate a four-class system classification in anesthesia from this related study in comparison with several CNN models.

As revealed in the aforementioned details, PPG, as one of the vital signs, is highly potentially able to estimate the blood pressure system. In further, the AI method, especially the deep neural network has been very widely utilized in many area particularly medical related fields either in the classification or the regression system. Moreover, with the help of the GA, as the optimizer, the ensemble model of the deep learning algorithm is prospectively utilized. Hence, the aim of this paper is to investigate the generative continuous ABP using deep neural network models via deep convolutional autoencoder (DCAE) by utilizing only a single PPG sensor.

Finally, the GA will form the ensemble model from the evaluation of the cross-validation models.

2. Materials and Methods

This study has been approved by the Research Ethics Committee, National Taiwan University Hospital (NTUH) in Taiwan. Furthermore, the written informed consent was received for the permission by the patients. Totally, 18 patients dataset is used for the evaluation. The dataset is acquired using MP60 IntelliVue Patient Monitor (Koninklijke Philips N.V, Amsterdam, Netherlands) that is connected to a PC.

Regarding to the dataset and the deep learning evaluations. The sampling rate of the PPG and ABP is 128 Hz. The window size evaluation is based on each 5-second signal both the PPG and ABP. This phenomenon means that each 5-second PPG signal is able to predict the current 5-second of the ABP signal. The data in manually filtered based on its quality. In this study, the range of the data is limited between 10 mmHg and 250 mmHg. Some noisy ABP signals are likely affected by the high-frequency noise. The dataset is randomly divided into 85% and 15% respectively for the training and testing data. MATLAB R2014b (The MathWorks, Inc., Natick, Massachusetts, USA) is utilized for pre-processing the data and post-processing the results. TensorFlow (Ver. 1.15.2) [30] and Keras (Ver. 2.3.1) are utilized in Google Colaboratory (Google Inc., California, USA) for the deep learning training using Python 3.6. The training is conducted for 200 epochs with batch size of 16 with Adam optimizer [31]. The model checkpoint is also set for the training system. As well, the training data is shuffled. Finally, cross-validation (CV) method is conducted to investigate the model regularity.

The evaluations are conducted based on mean absolute error (MAE), root mean squared error (RMSE), and Pearson's linear correlation coefficient. These evaluations are given on Eqs. 1-3. The Pearson's linear correlation coefficient evaluates between the MP60, as the golden standard, and the generated continuous arterial blood pressures. It also investigates the systolic blood pressure (SBP) and diastolic blood pressure (DBP) values, by taking the maximum and minimum values from the continuous signal, respectively for SBP and DBP, between MP60 IntelliVue Patient Monitor and the models. The given error is in mmHg. The R_(x,y) value is in range between 0 and 1. The model and the reference are perfectly correlated when the given R_(x,y) value is equal to 1.

$$MAE = {}^{1}/_{n} \sum_{i=1}^{n} |x_i - y_i| \tag{1}$$

$$RMSE = \sqrt{{}^{1}/_{n} \sum_{i=1}^{n} (x_i - y_i)^2} \tag{2}$$

$$R_{x,y} = \frac{\sum_{i=1}^{n}(x_i - \bar{x})(y_i - \bar{y})}{[\sum_{i=1}^{n}(x_i - \bar{x})^2 \sum_{i=1}^{n}(y_i - \bar{y})^2]^{1/2}} \quad (3)$$

Where the x_i is the reference, y_i is the estimated result, n is the number of sample, $\bar{x}$ is the mean of the reference, and $\bar{y}$ is the mean of the estimated result.

This study evaluates two DCAE models. Basically, the autoencoder structure is shown in Figure 1. The first model is generated based on the LeNet-5 CNN model [32]. Originally, this model worked for the digit recognition system. The architecture of this model is relatively simple compared to other models. The convolution layer on this model is regularly followed by the subsampling. For the classification system, there are several fully connected layers installed to the network. This study uses only the convolution layer with the subsampling from the original LeNet-5 model to form the encoder. Meanwhile, the decoder utilizes the opposite way of the encoder. The detail of the LeNet-5 based deep convolutional autoencoder (LDCAE) utilized in this study can be seen on Table 1. From this table, it can be seen that the original 5 seconds of the 1-dimensional PPG signal and the sampling rate of 128 Hz, with size of 640 points, is used for the input layer. For the encoder, this study applies the increasing filter size. All convolution layers administer the rectified linear unit (ReLU) activation function, shown on Eq. 4. This structure also uses the same padding. After the input layer, for the encoder, the first convolution layer starts with 16 filters and ends with 64 filters. However, the decoder works with initially 64 filters to 16 filters. The output layer is equal to the input layer. This layer is the 5-second ABP signal. This model has equal total parameter and trainable parameter, which is about sixty thousand parameters.

$$f(x) = \max(0,x) \quad (4)$$

Another model is the deep convolutional autoencoder based on the U-Net architecture [33]. This model was originally applied for the biomedical segmentation. One of the uniqueness of the U-Net model is the concatenating between a layer in encoder and another layer in decoder that has the same feature map. The detail structure of the U-Net based convolutional autoencoder (UDCAE) used in this study can be seen on Table 2. In parallel with the LDCAE model, this model also has input size of 640 data point of the PPG. The encoder and decoder structures are also very identical the LDCAE. However, the first filter in the encoder has 32 filters and ends with 256 filters. In further, the concatenated layer filters in the decoder are formed by considering the filter from the encoder layer. The UDCAE also utilizes the ReLU activation function. This UDCAE model has equal total number of settings and trainable parameters, which are about three hundred

thousand parameters. These numbers of parameter are much bigger compared to the LDCAE structure.

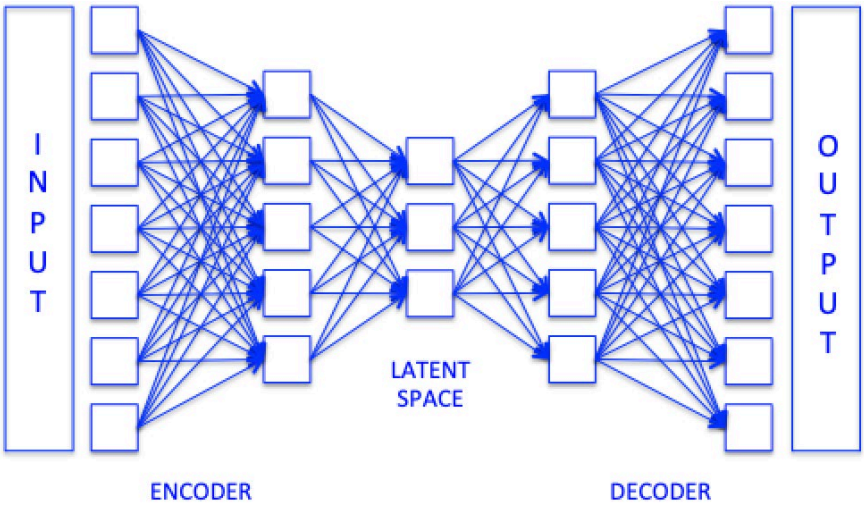

Figure 1. Basic autoencoder structure.

Table 1. LeNet-5 based deep convolution autoencoder (LDCAE) structure.

Layer (type)	Output Shape	Param #
input_1 (InputLayer)	(None, 640, 1)	0
CONV_01 (Conv1D)	(None, 640, 16)	64
D_POOL_01 (MaxPooling1D)	(None, 320, 16)	0
CONV_02 (Conv1D)	(None, 320, 16)	784
D_POOL_02 (MaxPooling1D)	(None, 160, 16)	0
CONV_03 (Conv1D)	(None, 160, 32)	1568
D_POOL_03 (MaxPooling1D)	(None, 80, 32)	0
CONV_04 (Conv1D)	(None, 80, 32)	3104
D_POOL_04 (MaxPooling1D)	(None, 40, 32)	0
CONV_05 (Conv1D)	(None, 40, 64)	6208
D_POOL_05 (MaxPooling1D)	(None, 20, 64)	0
CONV_06 (Conv1D)	(None, 20, 64)	12352
D_POOL_06 (MaxPooling1D)	(None, 10, 64)	0
CONV_07 (Conv1D)	(None, 10, 64)	12352
U_POOL_01 (UpSampling1D)	(None, 20, 64)	0
CONV_08 (Conv1D)	(None, 20, 64)	12352
U_POOL_02 (UpSampling1D)	(None, 40, 64)	0
CONV_09 (Conv1D)	(None, 40, 32)	6176
U_POOL_03 (UpSampling1D)	(None, 80, 32)	0
CONV_10 (Conv1D)	(None, 80, 32)	3104
U_POOL_04 (UpSampling1D)	(None, 160, 32)	0
CONV_11 (Conv1D)	(None, 160, 16)	1552
U_POOL_05 (UpSampling1D)	(None, 320, 16)	0

CONV_12 (Conv1D)	(None, 320, 1)	33
U_POOL_06 (UpSampling1D)	(None, 640, 1)	0

Table 2. U-Net based deep convolution autoencoder (UDCAE) structure.

Layer (type)	Output Shape	Param #	Connected to
INPUT (InputLayer)	(None, 640, 1)	0	
CONV_01 (Conv1D)	(None, 640, 32)	128	INPUT[0][0]
D_POOL_01 (MaxPooling1D)	(None, 320, 32)	0	CONV_01[0][0]
CONV_02 (Conv1D)	(None, 320, 32)	3104	D_POOL_01[0][0]
D_POOL_02 (MaxPooling1D)	(None, 160, 32)	0	CONV_02[0][0]
CONV_03 (Conv1D)	(None, 160, 64)	6208	D_POOL_02[0][0]
D_POOL_03 (MaxPooling1D)	(None, 80, 64)	0	CONV_03[0][0]
CONV_04 (Conv1D)	(None, 80, 64)	12352	D_POOL_03[0][0]
D_POOL_04 (MaxPooling1D)	(None, 40, 64)	0	CONV_04[0][0]
CONV_05 (Conv1D)	(None, 40, 128)	24704	D_POOL_04[0][0]
D_POOL_05 (MaxPooling1D)	(None, 20, 128)	0	CONV_05[0][0]
CONV_06 (Conv1D)	(None, 20, 128)	49280	D_POOL_05[0][0]
D_POOL_06 (MaxPooling1D)	(None, 10, 128)	0	CONV_06[0][0]
CONV_07 (Conv1D)	(None, 10, 128)	49280	D_POOL_06[0][0]
U_POOL_01 (UpSampling1D)	(None, 20, 128)	0	CONV_07[0][0]
CONC_01 (Concatenate)	(None, 20, 256)	0	CONV_06[0][0]
			U_POOL_01[0][0]
CONV_08 (Conv1D)	(None, 20, 128)	98432	CONC_01[0][0]
U_POOL_02 (UpSampling1D)	(None, 40, 128)	0	CONV_08[0][0]
CONC_02 (Concatenate)	(None, 40, 256)	0	CONV_05[0][0]
			U_POOL_02[0][0]
CONV_09 (Conv1D)	(None, 40, 64)	32832	CONC_02[0][0]
U_POOL_03 (UpSampling1D)	(None, 80, 64)	0	CONV_09[0][0]
CONC_03 (Concatenate)	(None, 80, 128)	0	CONV_04[0][0]
			U_POOL_03[0][0]
CONV_10 (Conv1D)	(None, 80, 64)	16448	CONC_03[0][0]
U_POOL_04 (UpSampling1D)	(None, 160, 64)	0	CONV_10[0][0]
CONC_04 (Concatenate)	(None, 160, 128)	0	CONV_03[0][0]
			U_POOL_04[0][0]
CONV_11 (Conv1D)	(None, 160, 32)	8224	CONC_04[0][0]
U_POOL_05 (UpSampling1D)	(None, 320, 32)	0	CONV_11[0][0]
CONC_05 (Concatenate)	(None, 320, 64)	0	CONV_02[0][0]
			U_POOL_05[0][0]
CONV_12 (Conv1D)	(None, 320, 32)	4128	CONC_05[0][0]
U_POOL_06 (UpSampling1D)	(None, 640, 32)	0	CONV_12[0][0]
CONC_06 (Concatenate)	(None, 640, 64)	0	CONV_01[0][0]
			U_POOL_06[0][0]

CONV_13 (Conv1D)	(None, 640, 1)	129	CONC_06[0][0]

Moreover, 10-fold cross-validation (CV) system is conducted to evaluate the data generalization to the models. This CV method uses leave one out cross-validation (LOOCV) technique, meaning that the CV model shuffles only the training part and keeps the testing data outside the shuffling system. The highest average BP of the CV fold, combining the DCAE models, is selected as the best single model.

Finally, this study deploys the genetic algorithm (GA) optimization method, named genetic deep autoencoder (GDCAE) to ensemble the ten CV models for each LDCAE and UDCAE. Each CV model has the equally distributed weight, meaning this each model will have the chance to be combined to other models. Therefore, this GA will have the total of 20 bits for each chromosome. The chromosome will contain the binary values. Zero means the model is not selected and one means the selected model. In further, this study uses 32 chromosomes, single point crossover system, 95% of mutation rate and 2000 generations. The GA fitness function equation is given by Eq. 5. This equation is a purely modified of Eq. 3. The Eq. 5 is also the average value of the Pearson's linear correlation coefficient between SBP and DBP, meaning that the weights are equally distributed.

$$\overline{R_{bp}} = \frac{1}{2}\left(\frac{\sum_{i=1}^{n}\left(x_{i,sbp} - \overline{x_{sbp}}\right)\left(y_{i,sbp} - \overline{y_{sbp}}\right)}{\left[\sum_{i=1}^{n}\left(x_{i,sbp} - \overline{x_{sbp}}\right)^2 \sum_{i=1}^{n}\left(y_{i,sbp} - \overline{y_{sbp}}\right)^2\right]^{1/2}} + \frac{\sum_{i=1}^{n}\left(x_{i,dbp} - \overline{x_{dbp}}\right)\left(y_{i,dbp} - \overline{y_{dbp}}\right)}{\left[\sum_{i=1}^{n}\left(x_{i,dbp} - \overline{x_{dbp}}\right)^2 \sum_{i=1}^{n}\left(y_{i,dbp} - \overline{y_{dbp}}\right)^2\right]^{1/2}} \right) \quad (5)$$

3. Results

This study utilizes the deep convolutional autoencoder (DCAE) models to generate the continuous arterial blood pressure signal (ABP) by using single photoplethysmography (PPG). The result produced by the models are compared to investigated the better model compared to the MP60 IntelliVue Patient Monitor as the golden standard. The evaluations cover the continuous arterial blood pressure signal and the systolic and diastolic blood pressures.

The training of the DCAE models can be seen on Figure 2. It can be seen that, for training, the UDCAE converges faster and better than the LDCAE. Furthermore, for the testing, the UDCAE model also provides a preferable result compared to the LDCAE. In addition, the UDCAE model shows relatively less fluctuation.

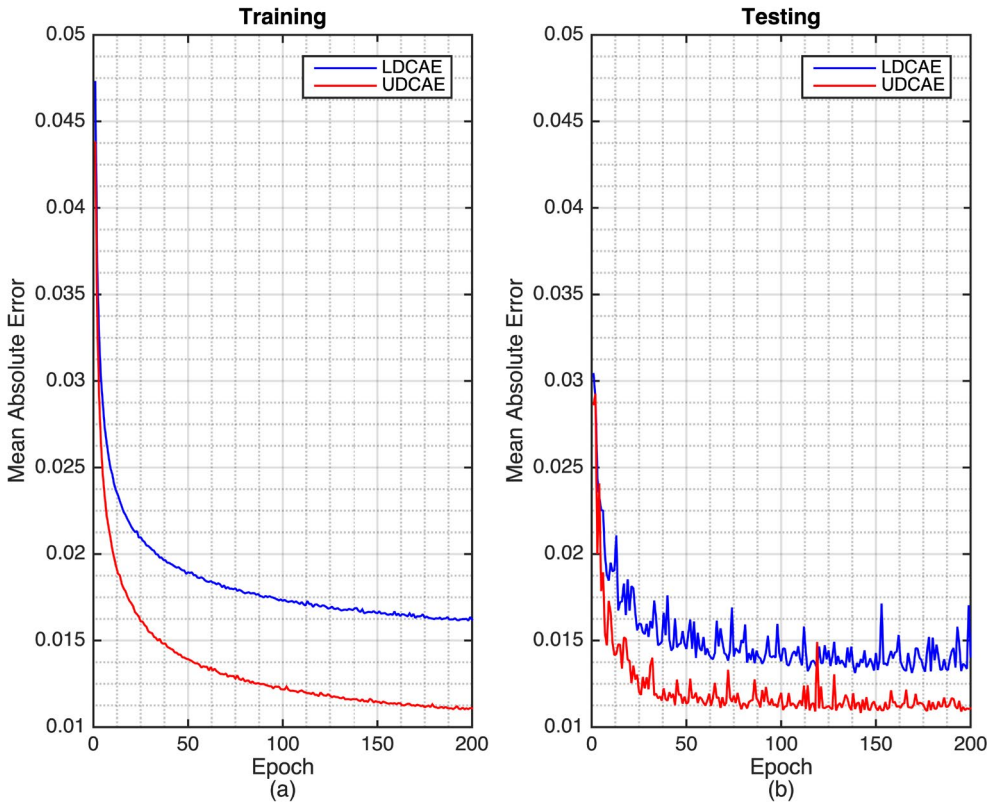

Figure 2. The training and testing of the LDCAE and UDCAE models.

Figure 3 shows the input of the PPG signal and its corresponding output of the continuous ABP signals, generated by the DCAE based models for the testing results. It can be seen that both models, LDCAE and UDCAE, successfully produce continuous ABP. In further, this figure also reveals the SBP and DBP can be accurately achieved. Both models display a fine estimation result in either the PPG has significant or non-significant second peak.

After performing the continuous ABP, the evaluation of SBP and DBP is further investigated. The maximum value of a 5-second segment is defined as the SBP. Meanwhile the minimum value is the DBP. This approach is deployed for both the DCAE models and the MP60, as the golden standard. The evaluation of the SBP and DBP can be seen on the error distribution on Figure 4. From this figure, both LDCAE and UDCAE are compared to the MP60 IntelliVue Patient Monitor values. It can be seen that the UDCAE model produces better outcomes by delivering more frequency result approaching to zero than the LDCAE model.

In further, to investigate the model prediction quality of the SBP and the DBP results compared to the MP60, another Pearson's linear correlation coefficient evaluation is performed. This estimation provides heterogeneous outcomes. The UDCAE has a slightly better result in envisaging the SBP prediction. Meanwhile, the LDCAE displays insignificantly better for the DBP estimation. The detail evaluation is shown in Figure 5.

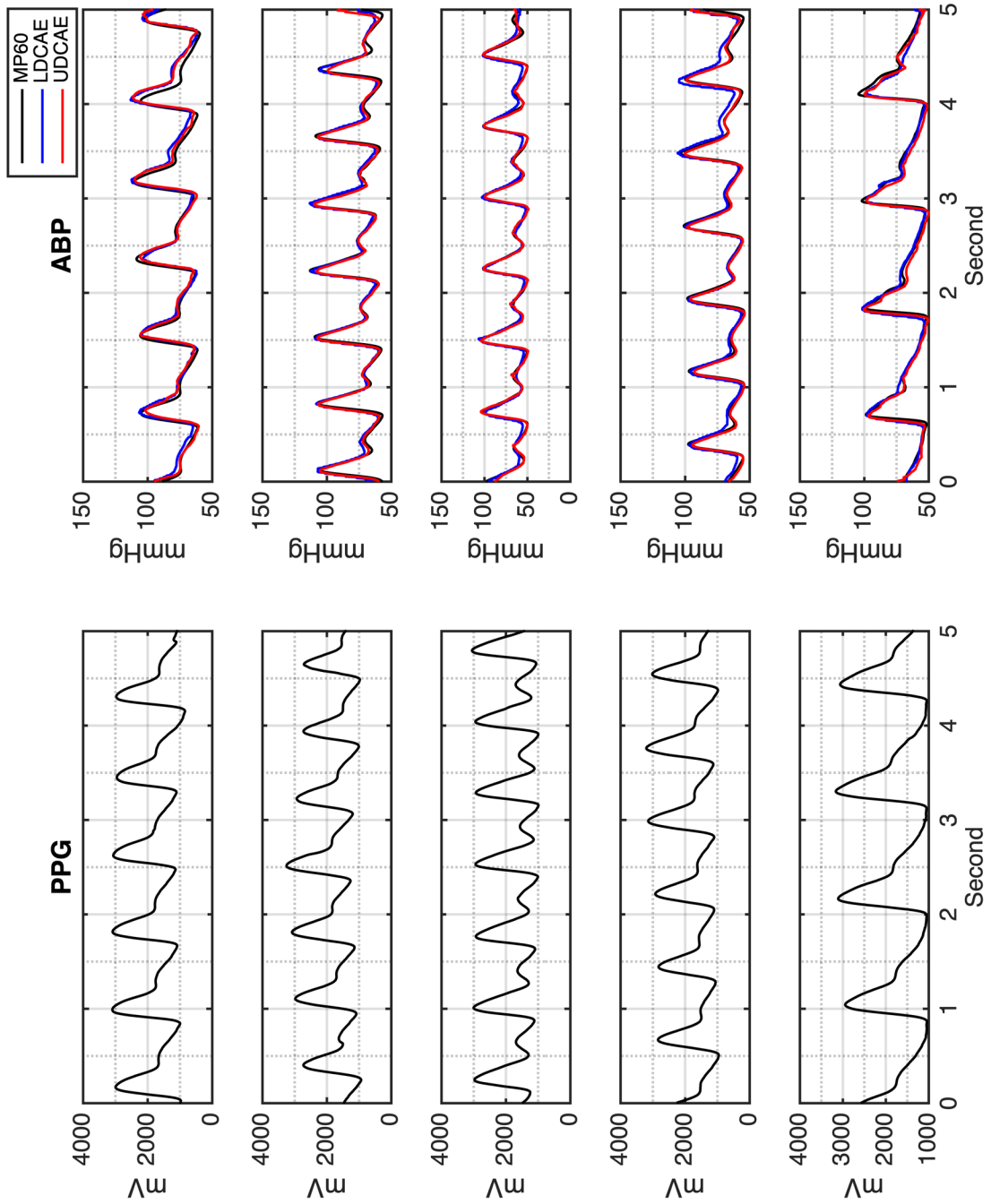

Figure 3. The PPG input signal and comparison results between LDCAE and UDCAE models and MP60 IntelliVue Patient Monitor.

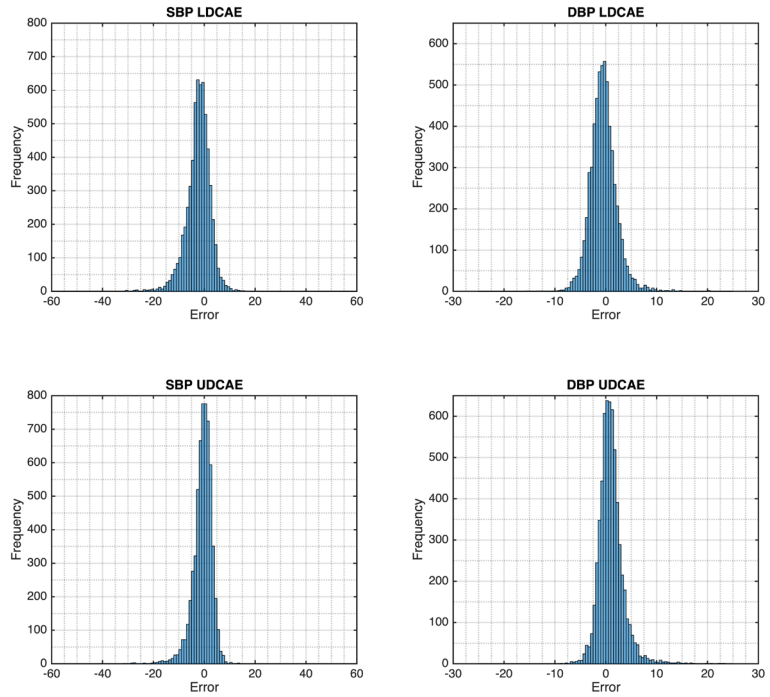

Figure 4. The error comparison between DCAE based models and MP60 IntelliVue Patient Monitor.

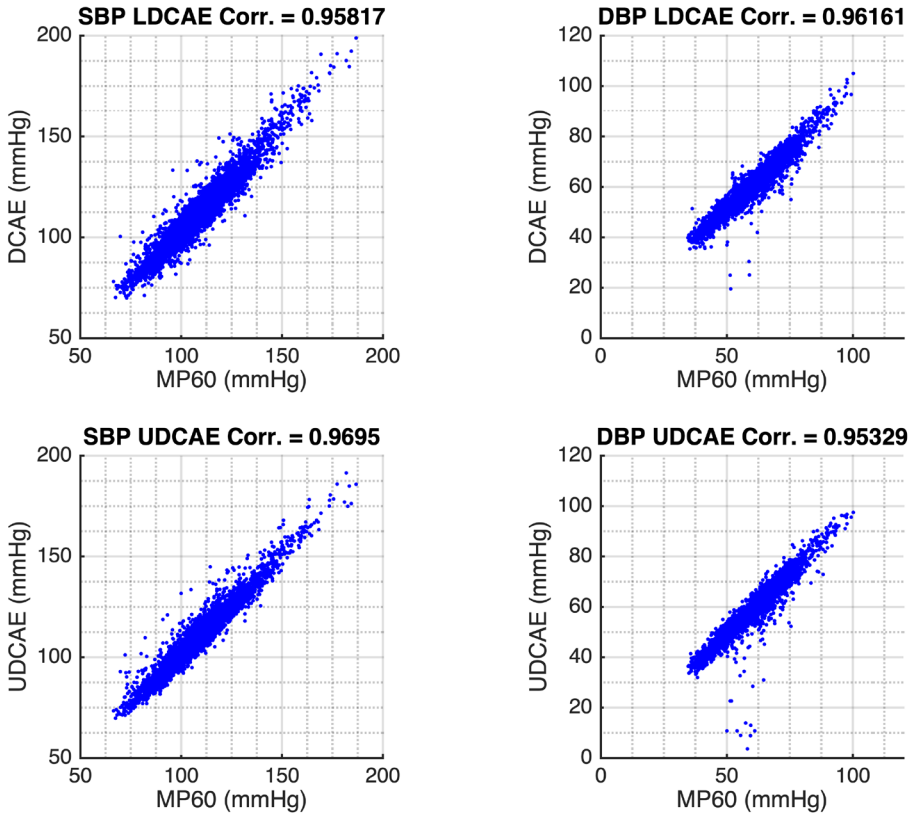

Figure 5. The Pearson's linear correlation comparison between DCAE based models and MP60 IntelliVue Patient Monitor.

Another powerful approach given by the DCAE models is the ability to generate the continuous ABP signal and is not interfered by any noise since the quality PPG is supplied. From Figure 6, it can be seen that some signals produced by the MP60 IntelliVue Patient Monitor are relatively noisy. However, the DCAE models are able to overcome it. Moreover, the predicted SBP and DBP values are comparable, by comparing them to either the preceding or the succeeding cycles.

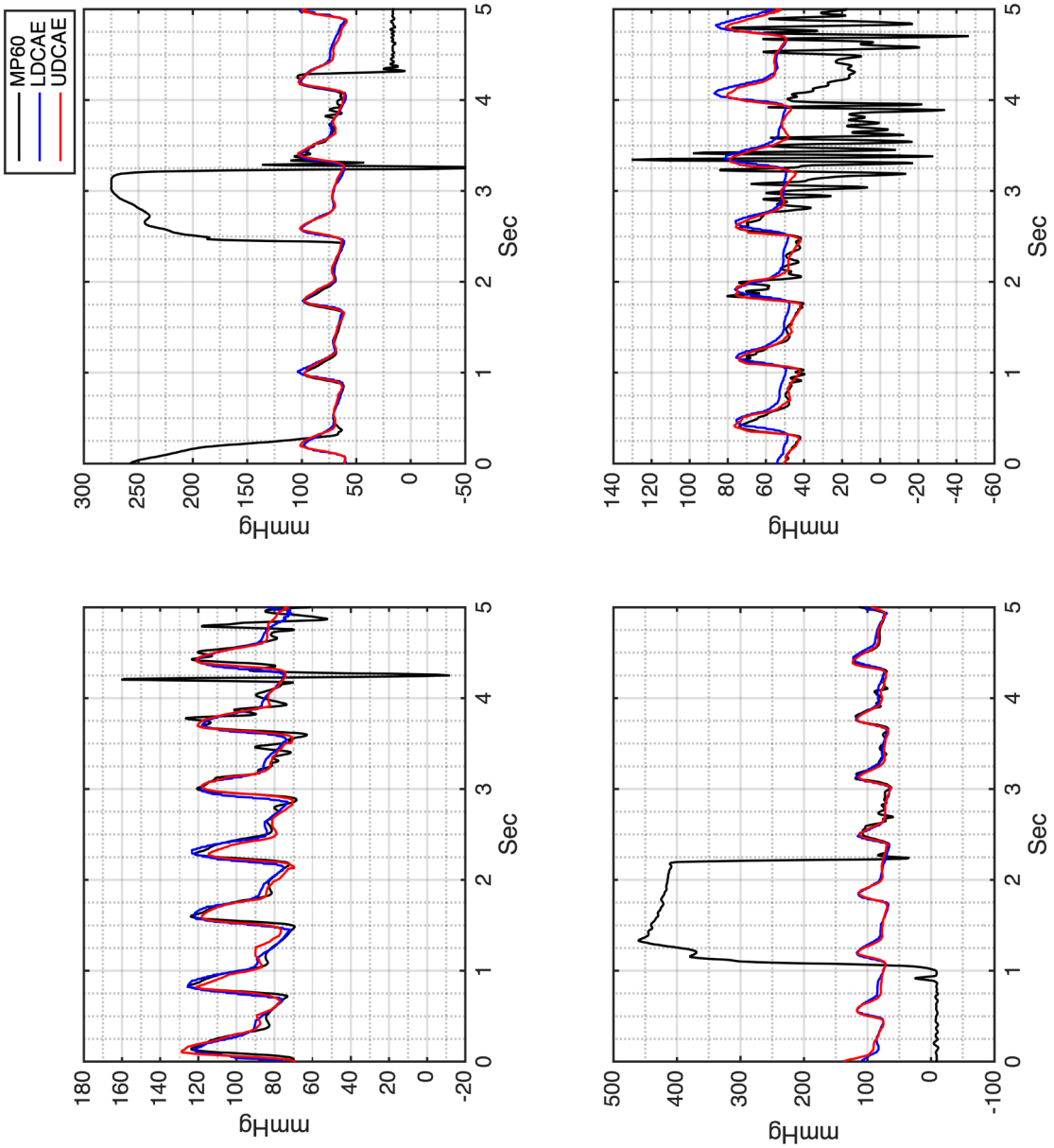

Figure 6. The comparison of the noisy MP60 ABP signal and the generated ABP signal by the LDCAE and UDCAE models.

The cross-validation is later performed in order to evaluate the data generalization and for the ensemble combination. The results show that the data has very high generalization. Good generalization is given by the standard deviation of the Pearson's linear correlation for the SBP, DBP and waveform evaluations, given in Table 3. Moreover, also the relatively small standard deviation of RMSE and MAE for the SBP, DBP and waveform evaluations are shown in Table 4.

The selection of the best single model from the CV results is evaluated based on the Pearson's linear correlation coefficient given in Table 3. It can be seen that the fourth CV model provides the highest average value between the SBP and DBP, which is 0.9643. Hence, this model is selected as the best single model.

Table 3. The Pearson's linear correlation coefficient evaluation of LDCAE and UDCAE models from cross-validation method. [Note: Bold value is the best single CV model].

CV	Correlation coefficient						
	SBP		DBP		Waveform		Average
	LDCAE	UDCAE	LDCAE	UDCAE	LDCAE	UDCAE	
1	0.956	0.958	0.958	0.953	0.968	0.974	0.9612
2	0.960	0.961	0.954	0.942	0.969	0.974	0.9600
3	0.962	0.965	0.951	0.941	0.968	0.975	0.9603
4	**0.958**	**0.969**	**0.962**	**0.953**	**0.968**	**0.976**	**0.9643**
5	0.954	0.964	0.963	0.962	0.966	0.975	0.9640
6	0.951	0.960	0.959	0.956	0.966	0.974	0.9610
7	0.956	0.957	0.947	0.951	0.967	0.973	0.9585
8	0.959	0.964	0.949	0.956	0.968	0.976	0.9620
9	0.957	0.963	0.947	0.946	0.966	0.975	0.9590
10	0.958	0.968	0.963	0.947	0.967	0.975	0.9630
Mean	0.957	0.963	0.955	0.951	0.967	0.975	
STD	0.003	0.004	0.007	0.007	0.001	0.001	

After having the CV models, both from LDACE and UDCAE, the genetic algorithm based optimization deep convolutional autoencoder (GDCAE) is subsequently performed. This GA will work as the selector of the DCAE models that will be combined for the ensemble system. As the result, the CV models 1, 2, 3, 4, 5 and 10 are selected by GA from the LDCAE model. Meanwhile, GA appoints all the UDCAE models, except the first model. The result also shows the reliability from the fourth model of the LDCAE and UDCAE systems.

Table 4. Error evaluations of SBP and DBP from LDCAE and UDCAE models.

CV	SBP						DBP					
	LDCAE			UDCAE			LDCAE			UDCAE		
	RMSE	STD	MAE	RMSE	STD	MAE	RMSE	STD	MAE	RMSE	STD	MAE
1	4.690	7.340	3.440	4.620	7.840	3.260	3.100	5.710	2.220	3.060	8.760	1.820
2	4.630	8.010	3.390	4.300	9.760	3.110	3.250	7.720	2.180	3.870	11.740	2.230
3	4.910	6.890	3.720	4.810	7.780	3.420	3.090	8.160	2.040	3.380	10.370	1.950
4	5.190	7.860	3.790	3.850	6.620	2.730	2.760	5.360	2.000	3.250	9.400	1.950
5	5.110	8.460	3.640	4.120	7.730	3.010	2.700	6.630	1.860	3.010	7.870	1.960
6	6.480	9.600	4.850	5.110	10.030	3.470	2.860	6.210	2.030	3.020	8.890	1.780
7	5.020	8.450	3.610	4.480	10.780	3.010	3.400	9.670	2.140	3.250	9.080	1.990
8	4.880	7.250	3.570	4.540	7.590	3.140	3.260	8.950	2.120	3.170	8.670	1.900
9	4.630	7.380	3.390	5.180	8.580	3.650	3.270	9.050	2.080	3.300	10.930	1.770
10	6.390	8.890	4.930	5.120	7.860	3.710	2.790	4.540	1.040	3.290	10.220	1.820
Mean	5.193	8.013	3.833	4.613	8.457	3.251	3.048	7.200	1.971	3.260	9.593	1.917
STD	0.682	0.843	0.573	0.449	1.310	0.310	0.252	1.756	0.343	0.249	1.188	0.136

CV	SBP						DBP					
	LDCAE			UDCAE			LDCAE			UDCAE		
	RMSE	STD	MAE	RMSE	STD	MAE	RMSE	STD	MAE	RMSE	STD	MAE
1	4.690	7.340	3.440	4.620	3.190	3.260	3.280	5.710	2.220	3.060	2.150	1.820
2	4.630	8.010	3.390	4.300	3.140	3.110	2.980	7.720	2.180	3.870	2.420	2.230
3	4.910	6.890	3.720	4.810	3.210	3.420	3.380	8.160	2.040	3.380	2.320	1.950
4	5.190	7.860	3.790	3.850	3.540	2.730	2.720	5.360	2.000	3.250	1.890	1.950
5	5.110	8.460	3.640	4.120	3.580	3.010	2.810	6.630	1.860	3.010	1.960	1.960
6	6.480	9.600	4.850	5.110	2.290	3.470	3.750	6.210	2.030	3.020	2.020	1.780
7	5.020	8.450	3.610	4.480	3.490	3.010	3.270	9.670	2.140	3.250	2.640	1.990
8	4.880	7.250	3.570	4.540	3.330	3.140	3.290	8.950	2.120	3.170	2.480	1.900
9	4.630	7.380	3.390	5.180	3.160	3.650	3.670	9.050	2.080	3.300	2.520	1.770
10	6.390	8.890	4.930	5.120	4.070	3.710	3.530	4.540	1.040	3.290	1.910	1.820
Mean	5.193	8.013	3.833	4.613	3.300	3.251	3.268	7.200	1.971	3.260	2.231	1.917
STD	0.682	0.843	0.573	0.449	0.454	0.310	0.345	1.756	0.343	0.249	0.279	0.136

CV	SBP						DBP					
	LDCAE			UDCAE			LDCAE			UDCAE		
	RMSE	STD	MAE	RMSE	STD	MAE	RMSE	STD	MAE	RMSE	STD	MAE
1	4.690	7.340	3.440	4.620	7.840	3.260	3.100	5.710	2.220	3.060	8.760	1.820
2	4.630	8.010	3.390	4.300	9.760	3.110	3.250	7.720	2.180	3.870	11.740	2.230
3	4.910	6.890	3.720	4.810	7.780	3.420	3.090	8.160	2.040	3.380	10.370	1.950
4	5.190	7.860	3.790	3.850	6.620	2.730	2.760	5.360	2.000	3.250	9.400	1.950
5	5.110	8.460	3.640	4.120	7.730	3.010	2.700	6.630	1.860	3.010	7.870	1.960
6	6.480	9.600	4.850	5.110	10.030	3.470	2.860	6.210	2.030	3.020	8.890	1.780
7	5.020	8.450	3.610	4.480	10.780	3.010	3.400	9.670	2.140	3.250	9.080	1.990
8	4.880	7.250	3.570	4.540	7.590	3.140	3.260	8.950	2.120	3.170	8.670	1.900
9	4.630	7.380	3.390	5.180	8.580	3.650	3.270	9.050	2.080	3.300	10.930	1.770
10	6.390	8.890	4.930	5.120	7.860	3.710	2.790	4.540	1.040	3.290	10.220	1.820
Mean	5.193	8.013	3.833	4.613	8.457	3.251	3.048	7.200	1.971	3.260	9.593	1.917
STD	0.682	0.843	0.573	0.449	1.310	0.310	0.252	1.756	0.343	0.249	1.188	0.136

CV	SBP						DBP					
	LDCAE			UDCAE			LDCAE			UDCAE		
	RMSE	STD	MAE	RMSE	STD	MAE	RMSE	STD	MAE	RMSE	STD	MAE
1	4.690	7.340	3.440	4.620	3.190	3.260	3.280	5.710	2.220	3.060	2.150	1.820
2	4.630	8.010	3.390	4.300	3.140	3.110	2.980	7.720	2.180	3.870	2.420	2.230
3	4.910	6.890	3.720	4.810	3.210	3.420	3.380	8.160	2.040	3.380	2.320	1.950
4	5.190	7.860	3.790	3.850	3.540	2.730	2.720	5.360	2.000	3.250	1.890	1.950
5	5.110	8.460	3.640	4.120	3.580	3.010	2.810	6.630	1.860	3.010	1.960	1.960
6	6.480	9.600	4.850	5.110	2.290	3.470	3.750	6.210	2.030	3.020	2.020	1.780
7	5.020	8.450	3.610	4.480	3.490	3.010	3.270	9.670	2.140	3.250	2.640	1.990
8	4.880	7.250	3.570	4.540	3.330	3.140	3.290	8.950	2.120	3.170	2.480	1.900
9	4.630	7.380	3.390	5.180	3.160	3.650	3.670	9.050	2.080	3.300	2.520	1.770
10	6.390	8.890	4.930	5.120	4.070	3.710	3.530	4.540	1.040	3.290	1.910	1.820
Mean	5.193	8.013	3.833	4.613	3.300	3.251	3.268	7.200	1.971	3.260	2.231	1.917
STD	0.682	0.843	0.573	0.449	0.454	0.310	0.345	1.756	0.343	0.249	0.279	0.136

The convergence of the GDCAE is shown in Figure 7. Several chromosome sizes of 4, 8, 16, 32 and 64 are investigated. The average result from the SBP and DBP of GDCAE is 0.980. This GDCAE result is better compared to the average value of SBP and DBP from best single CV model, 0.960 and 0.961 for LDCAE and UDCAE models, respectively. By having this combination, the GA-optimized reconstructed signal is later performed. The results also provide some improvements in comparison to the best CV model in Pearson's linear correlation coefficient and error evaluations, which can be seen in Table 5.

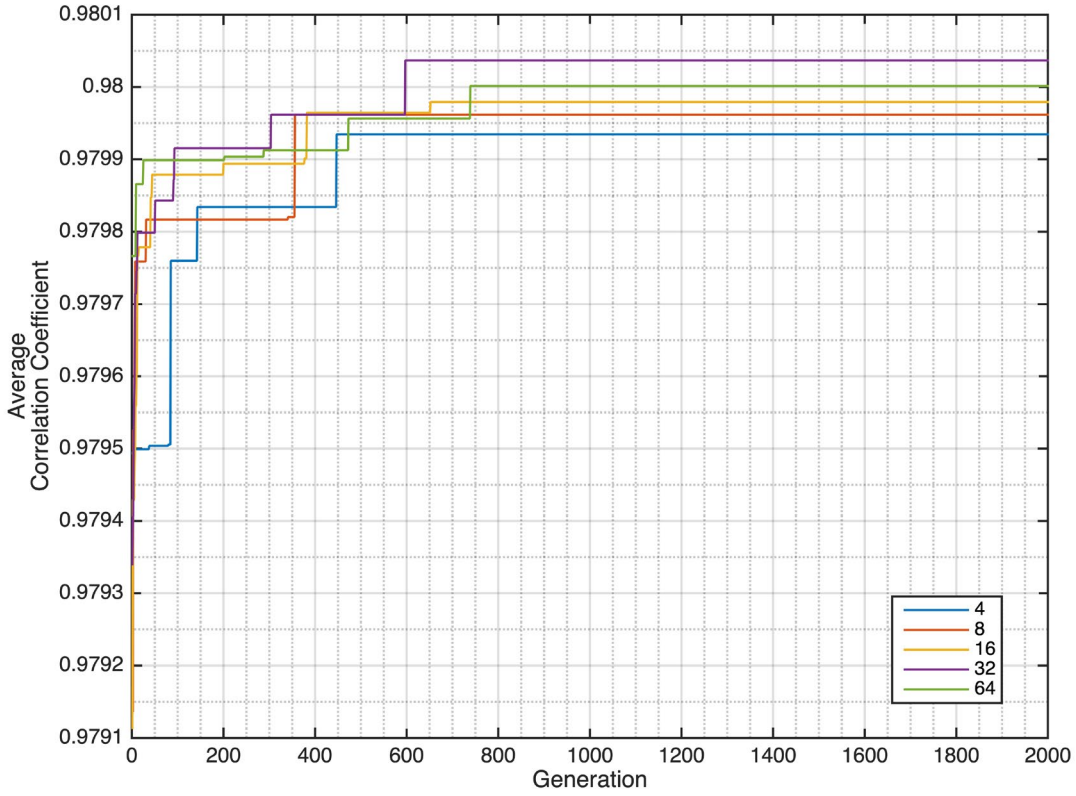

Figure 7. GDCAE generation convergence.

4. Discussion

Initially in this study, the PPG signal is trained by using DCAE models, LeNet and U-Net based models, to generate the continuous arterial blood pressure (ABP) signal. In this step, the PPG and MP60 IntelliVue Patient Monitor generated continuous arterial blood pressure signals are compared. Moreover, the systolic and diastolic blood pressures are evaluated by root mean squared error (RMSE) and the correlation coefficient between the models with the MP60 IntelliVue Patient Monitor as the golden standard. Finally, the GA regulated DCAE based on the cross-validation results is deployed to ensemble the model and evaluate the system.

Table 5. Comparison between LDCAE, UDCAE and GDCAE models.

Method	Correlation Coefficient			Error evaluations [mmHg]		
	Waveform	SBP	DBP	Waveform	SBP	DBP
LDCAE	R = 0.968	R = 0.958	R = 0.962	RMSE = 5.10 STD = 8.82 MAE = 3.52 STD = 3.69	RMSE = 5.19 STD = 7.86 MAE = 3.80 STD = 3.54	RMSE = 2.76 STD = 5.36 MAE = 2.00 STD = 1.89
UDACE	R = 0.976	R = 0.969	R = 0.953	RMSE = 4.25 STD = 8.78 MAE = 2.77 STD = 3.22	RMSE = 3.85 STD = 6.62 MAE = 2.73 STD = 2.72	RMSE = 3.25 STD = 9.40 MAE = 1.95 STD = 2.62
GDCAE	R = 0.984	R = 0.981	R = 0.979	RMSE = 3.46 STD = 6.25 MAE = 2.33 STD = 2.56	RMSE = 3.41 STD = 4.97 MAE = 2.54 STD = 2.74	RMSE = 2.14 STD = 4.63 MAE = 1.48 STD = 1.54

In order to investigate the quality of the proposed methods, the comparative study to the previously organized researches is conducted. The comparison method is included the dataset, input signal, methodology, generative system, error evaluations and linear correlations. The detail of the comparative studies is given in Table 6. Sideris et. al. [12] utilized the forty two patients dataset from MIMIC PhysioNet, originally two hundred dataset after applying some filtering steps based on the quality of the blood pressure signal. This study also only used the single PPG signal. The overlapped window size was used in order to form either the training or the testing. In further, the LSTM, one of the deep neural network methods, applied for the prediction. One of the essential achievements from this study is the ability to generate the continuous arterial blood pressure signal. As it can be seen, the capability of LSTM is able to produce the continuous arterial blood pressure by only utilizing the PPG signal. It, however, did not mention specifically about the RMSE of the DBP. Nevertheless, in this study they provided a table consisting the tabulated RMSE result of SBP, DBP and ABP. With full respect to all of the authors in this study [12], we re-evaluate the ABP and SBP results based on the corresponding table. This is conducted to recalculate the mean and standard deviation which found to be . very identical results to their reported results. Hence, we perform the DBP calculation, in parallel to the aforementioned method for the ABP and SBP calculations. The results of DBP, for mean and standard deviation, is 1.98±1.06 mmHg. In comparison to our study, this study has slightly better results in RMSEs of SBP and DBP error evaluations. However, our study, the GDCAE, provides a better outcome in the waveform error evaluation, which is 0.984. Moreover, our GDCAE also delivers a superior solution for the correlation coefficient for the

waveform evaluation. Meanwhile, Sideris et. al. [12] did not provide any information about the SBP and DBP correlation coefficient results.

Another study related to blood pressure evaluation was conducted by Tanveer et. al. [13]. This study applied multiple vital signs, which are ECG and PPG. This study used the dataset of thirty-nine patients, from originally ninety-three patients, of MIMIC I PhysioNet database. This study had 16-second and 40-second of window sizes, with 125 Hz of sampling frequency. This study also deployed the LSTM method, similar to the study performed by Sideris et. al. [12], alongside the ANN. This study provided an outstanding result in the error estimation in mmHg. Based on the combination of LSTM and ANN method, their study produced significantly small RMSEs, which are 1.26 mmHg and 0.73 mmHg, respectively for SBP and DBP. Moreover, the MAEs for the SBP and DBP are respectively 0.93 mmHg and 0.52 mmHg. Identical to the error evaluation, the Pearson's linear correlation coefficient evaluation is also an exceptional finding. The nearly perfectly correlated system is produced, which are 0.999 and 0.998 for the SBP and DBP, respectively. This result is produced by the longer size, which is the 40-second window size system. However, this method has a drawback. It did not provide the information about the generative continuous arterial blood pressure.

A study investigated by Zadi et. al. [14] used fifteen young subjects. This study evaluated the blood pressure based on two conditions, which are normal breath and breath hold. The autoregressive moving average (ARMA) was deployed the modeling. This study produced relatively good result. It has RMSEs of 7.21 mmHg and 5.12 mmHg, respectively for the systolic and diastolic blood pressure. However, neither correlation coefficient for waveform, SBP nor DBP was provided. Moreover, there was no available generative continuous ABP signal investigation.

The last comparative study is the finding by Eom et. al. [15]. This study was conducted on fifteen subjects. It used several vital signs, which are ECG, PPG and BCG. The 5-second window size was also used in this study. The combination of CNN, bidirectional gated recurrent unit (Bi-GRU) and attention mechanism. The result showed the produced MAEs and standard deviations are 4.06±4.04 mmHg and 3.33±3.42 mmHg, respectively for the SBP and DBP. However, this study has a disadvantage, which is no generative continuous blood pressure estimation was performed.

As it can be seen from the aforementioned information comparing our proposed methods to previously performed studies, our study shows assorted advantages. Our proposed methods, working based on the deep autoencoder and using only a single PPG signal, provide a leading achievement for correlation coefficient for the waveform of the generative continuous blood pressure signal. Additionally, our proposed methods produce highly correlated results of the estimated SBP and DBP to the MP60 IntelliVue Patient Monitor, as the golden standard.

Table 6. Comparative results for dataset and methodology between the proposed method and previous related studies.

Studies	Dataset	Input Signal	Method	Gen. Cont. ABP	Correlation Coefficient			Error Evaluations [mmHg]		
					Waveform	SBP	DBP	Waveform	SBP	DBP
Sideris et. al. [12]	42 subjects, MIMIC PhysioNet	PPG	LSTM	Yes	Mean = 0.95 STD = 0.045	N/A	N/A	RMSE = 6.04 STD = 3.26	RMSE = 2.58 STD = 1.23	RMSE = 1.98 STD = 1.06
Tanveer et. al. [13]	39 subjects, MIMIC PhysioNet	ECG + PPG	ANN + LSTM	No	N/A	0.999	0.998	N/A	RMSE = 1.26 MAE = 0.93	RMSE = 0.73 MAE = 0.52
Zadi et. al. [14]	15 subjects	PPG	ARMA	No	N/A	N/A	N/A	N/A	RMSE = 7.21	RMSE = 5.12
Eom et. al. [15]	15 subjects	ECG + PPG + BCG	CNN + Bi-GRU + Attention	No	N/A	$R^2 = 0.52$	$R^2 = 0.49$	N/A	MAE = 4.06 STD = 4.04	MAE = 3.33 STD = 3.42
Proposed	18 subjects, NTUH, Taiwan	PPG	LDCAE	Yes	R = 0.968	R = 0.958	R = 0.962	RMSE = 5.10 STD =8.82 MAE = 3.52 STD = 3.69	RMSE = 5.19 STD = 7.86 MAE = 3.80 STD = 3.54	RMSE = 2.76 STD = 5.36 MAE = 2.00 STD = 1.89
			UDCAE		R = 0.976	R = 0.969	R = 0.953	RMSE = 4.25 STD = 8.78 MAE = 2.77 STD = 3.22	RMSE = 3.85 STD = 6.62 MAE = 2.73 STD = 2.72	RMSE = 3.25 STD = 9.40 MAE = 1.95 STD = 2.62
			GDCAE		R = 0.984	R = 0.981	R = 0.979	RMSE = 3.46 STD = 6.25 MAE = 2.33 STD = 2.56	RMSE = 3.41 STD = 4.97 MAE = 2.54 STD = 2.74	RMSE = 2.14 STD = 4.63 MAE = 1.48 STD = 1.54

However, this study has several limitations. The number of the patients utilized in this study is relatively small. Furthermore, the algorithm to evaluate the SBP and the DBP from the 5-second sliding window can be improved. This technique is selected based on the consideration of either SBP or the DBP does not fluctuate significantly within five seconds. In addition, the noisy PPG will contribute to the low-quality continuous ABP prediction, as it can be seen in Figure 8.

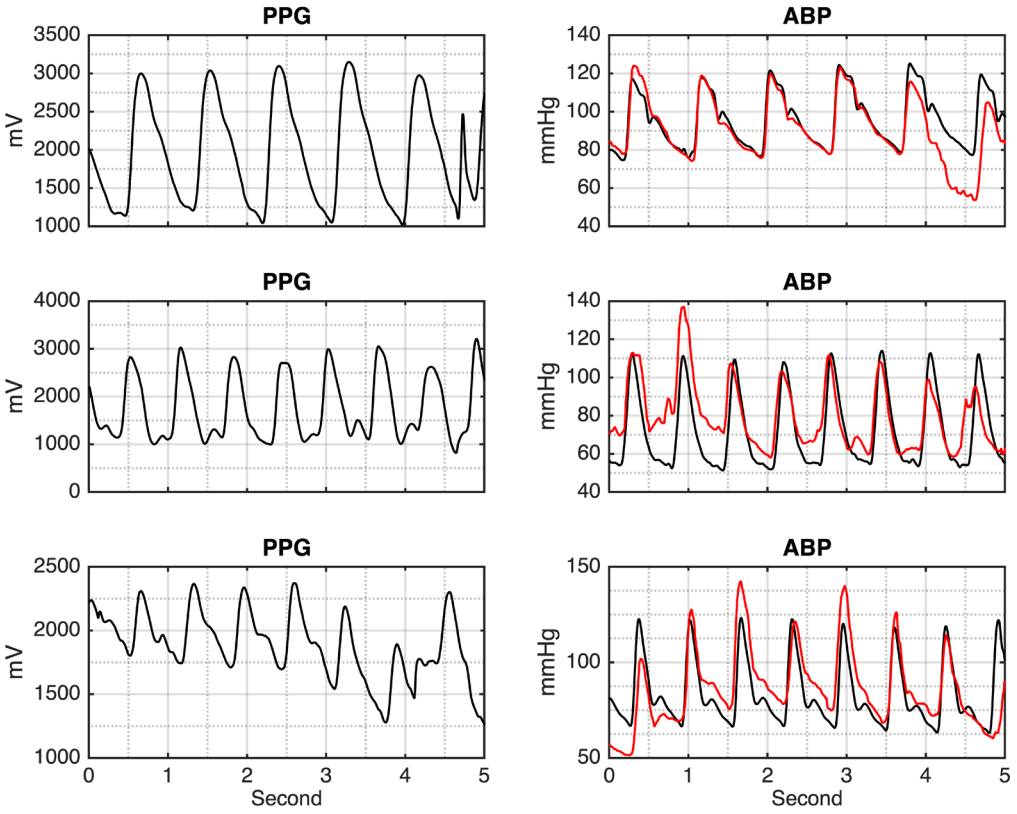

Figure 8. Low quality generated continuous ABP.

5. Conclusions

This study provides the consideration revealing that the deep convolutional autoencoder methods with the genetic algorithm based optimization has successfully evaluated the continuous arterial blood pressure system by only using a single PPG signal. In further, this study, supporting the previous studies, also shows straightforward information that the PPG is highly correlated to the continuous arterial blood pressure. Hence, the SBP and DBP measurements can be precisely achieved by only a single PPG signal.

References

1. Available online: https://www.who.int/news-room/fact-sheets/detail/hypertension (accessed on March 18th, 2020).
2. He, J. and Whelton, P.K. Elevated systolic blood pressure and risk of cardiovascular and renal disease: overview of evidence from observational epidemiologic studies and randomized controlled trials. *American heart journal* **1999**, 138(3), pp. S211-S219.
3. Lawes, C.M., Vander Hoorn, S. and Rodgers, A. Global burden of blood-pressure-related disease, 2001. *The Lancet* **2008**, 371(9623), pp.1513-1518.
4. Wong, T.Y. and McIntosh, R. Hypertensive retinopathy signs as risk indicators of cardiovascular morbidity and mortality. *British medical bulletin* **2005**, 73(1), pp.57-70.
5. Sadrawi, M., Shieh, J.S., Haraikawa, K., Chien, J.C., Lin, C.H. and Abbod, M.F. Ensemble empirical mode decomposition applied for PPG motion artifact. *In 2016 IEEE EMBS Conference on Biomedical Engineering and Sciences (IECBES)* **2016,** pp. 266-269. IEEE.
6. Tang, S.C., Huang, P.W., Hung, C.S., Shan, S.M., Lin, Y.H., Shieh, J.S., Lai, D.M., Wu, A.Y. and Jeng, J.S. Identification of atrial fibrillation by quantitative analyses of fingertip photoplethysmogram. *Scientific reports* **2017**, 7, p.45644.
7. Liang, Y., Chen, Z., Ward, R. and Elgendi, M. Hypertension assessment using photoplethysmography: a risk stratification approach. *Journal of clinical medicine* **2019**, 8(1), p.12.
8. Phillips, J.P., Hickey, M. and Kyriacou, P.A. Evaluation of electrical and optical plethysmography sensors for noninvasive monitoring of hemoglobin concentration. *Sensors* **2012**, 12(2), pp.1816-1826.
9. Perpetuini, D., Chiarelli, A.M., Cardone, D., Rinella, S., Massimino, S., Bianco, F., Bucciarelli, V., Vinciguerra, V., Fallica, G., Perciavalle, V. and Gallina, S. Photoplethysmographic Prediction of the Ankle-Brachial Pressure Index through a Machine Learning Approach. *Applied Sciences* **2020**, 10(6), p.2137.
10. Wei, H.C., Ta, N., Hu, W.R., Xiao, M.X., Tang, X.J., Haryadi, B., Liou, J.J. and Wu, H.T. Digital Volume Pulse Measured at the Fingertip as an Indicator of Diabetic Peripheral Neuropathy in the Aged and Diabetic. *Entropy* **2019**, 21(12), p.1229.
11. Sadrawi, M., Shieh, J.S., Fan, S.Z., Lin, C.H., Haraikawa, K., Chien, J.C. and Abbod, M.F. Intermittent blood pressure prediction via multiscale entropy and ensemble artificial neural networks. *In 2016 IEEE EMBS Conference on Biomedical Engineering and Sciences (IECBES)* **2016**, pp. 356-359. IEEE.
12. Sideris, C., Kalantarian, H., Nemati, E. and Sarrafzadeh, M. Building continuous arterial blood pressure prediction models using recurrent networks. *In 2016 IEEE International Conference on Smart Computing (SMARTCOMP)* **2016**, pp. 1-5. IEEE.
13. Tanveer, M.S. and Hasan, M.K. Cuffless blood pressure estimation from electrocardiogram and photoplethysmogram using waveform based ANN-LSTM network. *Biomedical Signal Processing and Control* **2019**, 51, pp.382-392.
14. Zadi, A.S., Alex, R., Zhang, R., Watenpaugh, D.E. and Behbehani, K. Arterial blood pressure feature estimation using photoplethysmography. *Computers in biology and medicine* **2018**, 102, pp.104-111.
15. Eom, H., Lee, D., Han, S., Hariyani, Y.S., Lim, Y., Sohn, I., Park, K. and Park, C. End-to-End Deep Learning Architecture for Continuous Blood Pressure Estimation Using Attention Mechanism. *Sensors* **2020**, 20(8), p.2338.
16. Sadrawi, M., Yunus, J., Khalil, M., Sofyan, S.E., Abbod, M.F. and Shieh, J.S. Computational Fluid Dynamics Based Fuzzy Control Optimization of Heat Exchanger via Genetic Algorithm. *In 2019 IEEE International Conference on Cybernetics and Computational Intelligence (CyberneticsCom)* **2019**, pp. 1-6. IEEE.
17. Silitonga, A.S., Shamsuddin, A.H., Mahlia, T.M.I., Milano, J., Kusumo, F., Siswantoro, J., Dharma, S., Sebayang, A.H., Masjuki, H.H. and Ong, H.C. Biodiesel synthesis from Ceiba pentandra oil by microwave irradiation-assisted transesterification: ELM modeling and optimization. *Renewable Energy* **2020**, 146, pp.1278-1291.
18. Song, C., Lee, S., Gu, B., Chang, I., Cho, G.Y., Baek, J.D. and Cha, S.W. A Study of Anode-Supported Solid Oxide Fuel Cell Modeling and Optimization Using Neural Network and Multi-Armed Bandit Algorithm. *Energies* **2020**, *13*(7), p.1621.
19. Zaidan, M.A., Harrison, R.F., Mills, A.R. and Fleming, P.J. Bayesian hierarchical models for aerospace gas turbine engine prognostics. *Expert Systems with Applications* **2015**, 42(1), pp.539-553.

20. Sadrawi, M., Fan, S.Z., Abbod, M.F., Jen, K.K. and Shieh, J.S. Computational depth of anesthesia via multiple vital signs based on artificial neural networks. *BioMed research international* **2015**, 2015.
21. Sadrawi, M., Lin, C.H., Lin, Y.T., Hsieh, Y., Kuo, C.C., Chien, J.C., Haraikawa, K., Abbod, M.F. and Shieh, J.S. Arrhythmia evaluation in wearable ECG devices. *Sensors* **2017**, 17(11), p.2445.
22. Liao, Y.H., Shih, C.H., Abbod, M.F., Shieh, J.S. and Hsiao, Y.J. Development of an E-nose system using machine learning methods to predict ventilator-associated pneumonia. *Microsystem Technologies* **2020**, pp.1-11.
23. Liao, Y.H., Wang, Z.C., Zhang, F.G., Abbod, M.F., Shih, C.H. and Shieh, J.S. Machine Learning Methods Applied to Predict Ventilator-Associated Pneumonia with Pseudomonas aeruginosa Infection via Sensor Array of Electronic Nose in Intensive Care Unit. *Sensors* **2019**, 19(8), p.1866.
24. Zhou, Z.H.; Wu, J.; Tang, W. Ensembling neural networks: Many could be better than all. *Artif. Intell.* 2002, 137, 239–263.
25. Sadrawi, M., Sun, W.Z., Ma, M.H.M., Yeh, Y.T., Abbod, M.F. and Shieh, J.S. Ensemble Genetic Fuzzy Neuro Model Applied for the Emergency Medical Service via Unbalanced Data Evaluation. *Symmetry* **2018**, 10(3), p.71.
26. LeCun, Y., Bengio, Y. and Hinton, G. Deep learning. *nature* **2015**, 521(7553), pp.436-444.
27. Hannun, A.Y., Rajpurkar, P., Haghpanahi, M., Tison, G.H., Bourn, C., Turakhia, M.P. and Ng, A.Y. Cardiologist-level arrhythmia detection and classification in ambulatory electrocardiograms using a deep neural network. *Nature medicine* **2019**, 25(1), p.65.
28. Acharya, U.R., Oh, S.L., Hagiwara, Y., Tan, J.H. and Adeli, H. Deep convolutional neural network for the automated detection and diagnosis of seizure using EEG signals. *Computers in biology and medicine* **2018**, 100, pp.270-278.
29. Liu, Q., Cai, J., Fan, S.Z., Abbod, M.F., Shieh, J.S., Kung, Y. and Lin, L. Spectrum Analysis of EEG Signals Using CNN to Model Patient's Consciousness Level Based on Anesthesiologists' Experience. *IEEE Access* **2019**, 7, pp.53731-53742.
30. Abadi, M., Barham, P., Chen, J., Chen, Z., Davis, A., Dean, J., Devin, M., Ghemawat, S., Irving, G., Isard, M. and Kudlur, M. Tensorflow: A system for large-scale machine learning. *In 12th {USENIX} Symposium on Operating Systems Design and Implementation ({OSDI} 16*) **2016,** (pp. 265-283).
31. Kingma, D.P. and Ba, J. Adam: A method for stochastic optimization. *arXiv preprint* **2014,** arXiv:1412.6980.
32. LeCun, Y., Bottou, L., Bengio, Y. and Haffner, P. Gradient-based learning applied to document recognition. *Proceedings of the IEEE* **1998**, 86(11), pp.2278-2324.
33. Ronneberger, O., Fischer, P. and Brox, T. U-net: Convolutional networks for biomedical image segmentation. *In International Conference on Medical image computing and computer-assisted intervention (pp. 234-241)* **2015**. Springer, Cham.

Author Contributions: Conceptualization, J.S.S., M.S., and Y.T.L.; methodology, M.S., J.S.S. and M.F.A.; software, J.S.S., M.S., M.F.A., C.H.L and Y.T.L; validation, J.S.S., M.S., C.H.L, Y.H and Y.T.L; formal analysis, M.S.; investigation, J.S.S., M.S., Y.H and Y.T.L.; writing—original draft preparation, M.S., B.M, J.S.S. and M.F.A.; writing—review and editing, M.S., J.S.S. and M.F.A.; visualization, M.S.; supervision, J.S.S., M.F.A., S.Z.F, and Y.T.L. All authors have read and agreed to the published version of the manuscript.

Acknowledgments: In this section you can acknowledge any support given which is not covered by the author contribution or funding sections. This may include administrative and technical support, or donations in kind (e.g., materials used for experiments).

Conflicts of Interest: The authors declare no conflict of interest.